[*] Presently at NASA Manned Spacecraft Center, Space Physics Division, Houston, Texas.

[†] Presently at the University of Salford, Salford, England.

[1] W. R. S. Garton and K. Codling, Proc. Phys. Soc. (London) 75, 87 (1959).

[2] W. R. S. Garton, W. H. Parkinson, and E. M. Reeves, Proc. Phys. Soc. (London) 80, 860 (1962).

[3] R. D. Hudson, Phys. Rev. 135, 1212 (1964).

[4] R. D. Hudson and V. L. Carter, Phys. Rev. 137, 1648 (1965).

[5] R. E. Honig, RCA Rev. 23, 567 (1962).

[6] A. N. Nesmeyanov, in *Vapor Pressure of the Chemical Elements*, edited by Robert Gary (Elsevier, New York, 1963).

[7] R. Hultgren, R. L. Orr, P. D. Anderson, and K. K. Kelley, *Selected Values of Thermodynamic Properties of Metals and Alloys* (Wiley, New York, 1963).

[8] R. D. Hudson and V. L. Carter, J. Opt. Soc. Am. 58, 227 (1968).

[9] U. Fano, Phys. Rev. 124, 1866 (1961).

[10] P. L. Altick, Phys. Rev. 169, 21 (1968).

PHYSICAL REVIEW A VOLUME 2, NUMBER 3 SEPTEMBER 1970

Light Propagation in Optically Pumped Alkali Vapors[*]

B. S. Mathur,[†] H. Y. Tang, and W. Happer
Columbia Radiation Laboratory and Department of Physics, Columbia University, New York, New York 10027

(Received 28 January 1970)

The propagation of light in an optically pumped vapor is determined semiclassically by the expectation value of a dielectric susceptibility operator. We present explicit formulas for the dielectric susceptibility of a vapor of alkali atoms. The qualitative features of the susceptibility are illustrated for the specific case of Rb^{87}. The theory of this paper is essential for a clear understanding of phenomena such as the birefringence of alkali vapors and the microwave modulation of light by alkali vapors. Some experimental observations of birefringence in rubidium vapor are interpreted with the semiclassical theory.

I. INTRODUCTION

The purpose of this paper is to present a rigorous theory of light propagation in optically pumped alkali vapors. A complete analysis of light propagation is rather involved because the index of refraction of the vapor may be anisotropic, inhomogeneous, rapidly varying, and lossy. The most important shortcoming of simplified theories is that they do not adequately account for the spectral profile of the light beam. The spectral profile of the light beam is usually assumed to be much broader than the width of the atomic absorption lines. Under these conditions, theory predicts that alkali vapors should exhibit no birefringence.[1,2] However, birefringence is often observed experimentally in rubidium and cesium vapors.[3,4] A further inadequacy of simple theories occurs when there is microwave coherence in atomic vapors.[5] The spectral profile of a light beam which has passed through a vapor with microwave coherence is radically modified since sidebands, displaced by the microwave frequency, are added to the optical carrier waves. In rubidium and cesium, the displacement of these sidebands from the carrier can be significantly greater than the spectral widths of a typical lamp line.

Recently, several comprehensive theories have been developed to account for some of the phenomena mentioned above.[6,7] In this paper we shall follow the Happer-Mathur semiclassical theory,[6] hereafter referred to as HM. In this theory the propagation of a light wave through a vapor is governed by the dielectric susceptibility of the vapor. The basic theory of light propagation through optically pumped vapors is developed in Sec. II.

The susceptibility is not a constant, but it depends on the state of the vapor. Consequently, one must think of the susceptibility as the quantum-mechanical expectation value of a susceptibility operator. Explicit formulas for the susceptibility operator of an alkali atom are given in Sec. III.

As an example of the application of this theory to concrete problems, the results of some new experiments on the birefringence of rubidium vapor are analyzed in Sec. IV.

II. THEORY

We can think of a light beam as being composed of many monochromatic waves whose electric fields $\vec{E}$ may be written in the form

$$\vec{E} = \vec{\mathscr{E}}(\zeta, t)\exp[i(\vec{k}\cdot\vec{r} - \omega t)] + \text{c.c.} \quad , \tag{1}$$

where c.c. denotes complex conjugate. The amplitude $\vec{\mathscr{E}}$ will be a slowly varying function of time t and of distance ζ along the direction of propagation, where

$$\zeta = (1/k)\vec{k}\cdot\vec{r} \quad . \tag{2}$$

The oscillating electric field of the light will induce an oscillating electric dipole moment $\vec{p}$ in each atom of the vapor with

$$\vec{p} = \vec{\wp}\exp i(\vec{k}\cdot\vec{r} - \omega t) + \text{c.c.} \tag{3}$$

We shall always be concerned with weak light sources, that is, with sources for which the rates of induced adsorption are much smaller than the corresponding spontaneous decay rates. Then the dipole-moment amplitude $\vec{\wp}$ is directly proportional to the electric field amplitude, thus,

$$\vec{\wp} = \langle\overleftrightarrow{\alpha}\rangle\vec{\mathscr{E}} \quad . \tag{4}$$

The polarizability dyadic of the atom is denoted by $\langle\overleftrightarrow{\alpha}\rangle$. The polarizability is the expectation value of a ground-state operator:

$$\langle\overleftrightarrow{\alpha}\rangle = \mathrm{Tr}[\overleftrightarrow{\alpha}\rho] \quad . \tag{5}$$

Here ρ is the density matrix of the atomic ground state.

The density matrix may contain rapidly oscillating off-diagonal matrix elements or "coherences." In consequence, both $\langle\overleftrightarrow{\alpha}\rangle$ and $\vec{\wp}$ may contain components which oscillate at one of the ground-state transition frequencies. That is, even though an atom is driven by a monochromatic light wave, the induced polarization need not oscillate at the optical frequency alone. It may oscillate at the driving frequency plus and minus multiples of the atomic coherence frequencies.

The macroscopic polarization of the vapor is

$$\vec{P} = N\vec{p} = \vec{\mathscr{P}}\exp[i(\vec{k}\cdot\vec{r} - \omega t)] + \text{c.c.} \tag{6}$$

Here N is the atomic-number density. If we define the susceptibility operator by

$$\overleftrightarrow{\chi} = N\overleftrightarrow{\alpha} \quad , \tag{7}$$

we can use (6) and (4) to write

$$\vec{\mathscr{P}} = \langle\overleftrightarrow{\chi}\rangle\vec{\mathscr{E}} \quad . \tag{8}$$

Thus, the susceptibility is the polarizability per unit volume or, alternatively, the polarizability is the susceptibility per atom.

Suppose that microwave coherence exists in the vapor so that the susceptibility is a rapidly oscillating function of time. Then it is convenient to write the susceptibility in the form

$$\langle\overleftrightarrow{\chi}(\omega, \zeta, t)\rangle = \sum_{\omega'}\langle\omega'|\overleftrightarrow{\chi}|\omega\rangle\exp\{i[(k' - k)\zeta - (\omega' - \omega)t]\} \quad . \tag{9}$$

The sum over ω' is such that all coherence frequencies of the vapor are included in the set of difference frequencies $\omega - \omega'$. Hence, $\langle\omega|\overleftrightarrow{\chi}|\omega'\rangle$ can be chosen to be time independent, although it may still depend on the position ζ. One can think of $\langle\omega'|\overleftrightarrow{\chi}|\omega\rangle$ as a matrix element in the frequency domain; $\langle\omega'|\overleftrightarrow{\chi}|\omega\rangle$ couples two light waves of frequencies ω and ω'.

Now let us represent the electric field of a light wave as a superposition of many monochromatic waves. Then,

$$\vec{E} = \sum_{\omega}\vec{\mathscr{E}}(\omega)\exp[i(k\zeta - \omega t)] + \text{c.c.} \tag{10}$$

The problem one must solve is the following: Given the amplitudes $\mathscr{E}(\omega; \zeta_0, t_0)$ at some initial position ζ_0 and time t_0, how does one calculate the amplitudes $\mathscr{E}(\omega, \zeta_1 t_1)$ at some more distant position ζ_1 and later time t_1? In order to solve this problem, we introduce new independent variables

$$\xi = \tfrac{1}{2}(\zeta + ct) \quad , \tag{11}$$

$$\eta = \tfrac{1}{2}(\zeta - ct) \quad . \tag{12}$$

Then it can be shown[8] that the electric field amplitudes satisfy the set of coupled equations (sometimes called the reduced Maxwell's equations[9])

$$\frac{\partial\vec{\mathscr{E}}(\omega)}{\partial\xi} = 2\pi ik\sum_{\omega'}\langle\omega|\overleftrightarrow{\chi}_{\perp}|\omega'\rangle\cdot\vec{\mathscr{E}}(\omega') \quad . \tag{13}$$

The variable η is held constant in (13). Note that one uses the transverse susceptibility $\langle\omega|\overleftrightarrow{\chi}_{\perp}|\omega'\rangle$ in (13). If we define a transverse projection operator by

$$\overleftrightarrow{T}(\hat{k}) = \overleftrightarrow{1} - \hat{k}\hat{k} \quad , \tag{14}$$

then

$$\langle\omega|\overleftrightarrow{\chi}_{\perp}|\omega'\rangle = \overleftrightarrow{T}(\hat{k})\cdot\langle\omega|\overleftrightarrow{\chi}|\omega'\rangle\cdot\overleftrightarrow{T}(\hat{k}) \quad . \tag{15}$$

Physically, it is clear that only the transverse components of the susceptibility can affect the propagation of the light, since the longitudinal components of $\overleftrightarrow{\chi}$ give rise to longitudinal components of polarization, and dipole oscillators do not radiate in the direction of oscillation.

The coupled equations (13) are similar to the Schrödinger equation for a quantum-mechanical system, and they may be solved in the same way. The solution to (13) may be written in the form

$$\vec{\mathscr{E}}(\omega, \xi_1) = \sum_{\omega'}\overleftrightarrow{V}(\omega\xi_1; \omega'\xi_0)\cdot\vec{\mathscr{E}}(\omega'\xi_0) \quad . \tag{16}$$

Here the propagation matrix $\overleftrightarrow{V}$ is analogous to the time-evolution operator of elementary quantum mechanics. In analogy to quantum mechanics,[6] we can write a perturbation series expansion for $\overleftrightarrow{\mathrm{V}}$:

$$\overleftrightarrow{\mathrm{V}}(\omega\xi_1;\omega'\xi_0)=\overleftrightarrow{\delta}_{\omega\omega'}+2\pi ik\int_{\xi_0}^{\xi_1}\langle\omega|\overleftrightarrow{\chi_\perp}(\xi)|\omega'\rangle\,d\xi+(2\pi ik)^2\int_{\xi_0}^{\xi_1}d\xi\int_{\xi_0}^{\xi}d\xi'\times\sum_{\omega''}\langle\omega|\overleftrightarrow{\chi_\perp}(\xi)|\omega''\rangle\cdot\langle\omega''|\overleftrightarrow{\chi_\perp}(\xi')|\omega'\rangle+\cdots\ . \tag{17}$$

A. Optically Thin Vapors

Suppose that the vapor is optically thin, i.e., that

$$|(\xi_1-\xi_0)k\langle\omega|\overleftrightarrow{\chi_\perp}|\omega'\rangle|\ll 1\ . \tag{18}$$

Then one can neglect quadratic and higher-order terms in χ, and Eq. (17) becomes

$$\overleftrightarrow{\mathrm{V}}(\omega\xi_1;\omega'\xi_0)=\overleftrightarrow{\delta}_{\omega\omega'}+2\pi ik\int_{\xi_0}^{\xi_1}\langle\omega|\overleftrightarrow{\chi_\perp}(\xi)|\omega'\rangle\,d\xi\ . \tag{19}$$

Equation (19) is a good first approximation to many experimental situations.

B. Static Homogeneous Susceptibilities; Wave Surfaces

Let us consider the case where the susceptibility is static or very slowly varying. Then, electric field amplitudes of different frequencies will not be coupled and the susceptibility matrix elements become

$$\langle\omega|\overleftrightarrow{\chi_\perp}|\omega'\rangle=\delta_{\omega\omega'}\langle\overleftrightarrow{\chi_\perp}(\omega)\rangle\ . \tag{20}$$

We shall also assume that $\langle\chi_\perp(\omega)\rangle$ is independent of ξ, i.e., we assume that the susceptibility is spatially homogeneous. Under these conditions, Eq. (17) becomes

$$\overleftrightarrow{\mathrm{V}}(\omega\xi_1;\omega'\xi_0)=\delta_{\omega\omega'}\exp[2\pi ik(\zeta_1-\zeta_0)\langle\overleftrightarrow{\chi_\perp}(\omega)\rangle]\ . \tag{21}$$

That is, the propagation matrix describes attenuation and changes in polarization of the light wave, but not frequency changes. From (21) and (16) we find that the electric field for a light wave in the vapor has the form

$$\vec{E}(\zeta,t)=\exp[i(\overleftrightarrow{\mathrm{K}}\zeta-\omega t)]\,\vec{\mathcal{E}}(0,t)+\text{c.c.} \tag{22}$$

The complex propagation dyadic $\overleftrightarrow{\mathrm{K}}$ is

$$\overleftrightarrow{\mathrm{K}}=k\overleftrightarrow{\mathrm{n}}\ , \tag{23}$$

where $\overleftrightarrow{\mathrm{n}}$ is the index-of-refraction dyadic

$$\overleftrightarrow{\mathrm{n}}=\overleftrightarrow{1}+2\pi\langle\overleftrightarrow{\chi_\perp}\rangle\ . \tag{24}$$

The propagation dyadic will always have two transverse eigenvectors $\vec{e}_\lambda$:

$$\overleftrightarrow{\mathrm{K}}\cdot\vec{e}_\lambda=k_\lambda\vec{e}_\lambda\quad(\lambda=1,2)\ . \tag{25}$$

These eigenvectors represent the polarizations of of the two wave surfaces[10] of the vapor. The eigenvalues k_λ determine the complex phase velocities v_λ of the two eigenwaves:

$$v_\lambda=\omega/k_\lambda\ . \tag{26}$$

The real part of v_λ determines the actual phase velocity of the wave, and the imaginary part of v_λ determines the rate of attenuation of the wave.

A widespread and convenient representation of light propagation in anisotropic media makes use of wave surfaces.[10] The normal-velocity surface is simply a plot of the phase velocity v_λ as a function of the direction of propagation. The ray-velocity surface is the surface which would be obtained if a short pulse of light were set off at some point in the vapor and if the resulting wave front were allowed to expand in all directions. It is worth noting that the ray-velocity surface and the normal-velocity surface are identical to first order in $\langle\chi\rangle$. Since we shall always be concerned with susceptibilities which are much smaller than unity, we can use the ray-velocity surface and the normal-velocity surface interchangeably. Both surfaces will be referred to as "the wave surface."

If the susceptibility is time dependent, we must, in general, solve the full propagation equation (13). However, we may use the instantaneous value of $\langle\chi\rangle$ in (22) if both of the following conditions are satisfied. Firstly, the susceptibility must not change appreciably during the time required by the light to pass through the vapor. Second, it is essential that no appreciable variation of $\langle\chi_\perp(\omega)\rangle$ occur over the frequency range occupied by the sidebands of the light wave. From (13) we find that the latter criterion is satisfied provided that

$$2\pi k\zeta\,|\langle\chi_\perp(\omega_0)\rangle|\,\omega_m/\Delta\omega_D\ll 1\ . \tag{27}$$

Here ζ is the thickness of the vapor; $|\langle\chi_\perp(\omega_0)\rangle|$ is the amplitude of the oscillating susceptibility, evaluated at the optical carrier frequency ω_0; and ω_m is the oscillation frequency of $\langle\chi_\perp(\omega_0)\rangle$. The Doppler width of the atomic absorption line is denoted by $\Delta\omega_D$.

C. Light with Broad Spectral Profile

Optical-pumping experiments are usually done with incoherent light from a resonance lamp. The light from such a lamp will be characterized by some spectral profile function $\Phi(\nu)=2\pi\Phi(\omega)$ such that $\Phi(\nu)d\nu$ is the energy flux carried by the light waves whose frequencies lie between ν and $\nu+d\nu$. Such light can be represented by an ensemble of many monochromatic waves of random phases. The average energy flux carried by a monochromatic light wave is

$$\Phi = (c/4\pi)\langle|\vec{E}|^2\rangle_{\mathrm{av}} \;, \tag{28}$$

where the symbol "av" denotes an average over several optical cycles. For a superposition of monochromatic waves such as (10), one can always make the replacement

$$\int \Phi(\omega)d\omega = (c/2\pi)\sum_{\omega}|\vec{\mathcal{E}}(\omega)|^2 \;. \tag{29}$$

Occasionally, one does experiments in which the incident light is already modulated in some way.[11] Under such conditions one must retain phase relations between different frequency components of the incident light wave, and it is not sufficient to specify only the spectral profile $\Phi(\nu)$. It is not difficult to treat the case of modulated incident light, but we shall not consider it further here.

D. Attenuation of Light Beam

Let us assume that light of a definite polarization vector $\vec{e}$ and initial spectral profile $\Phi(\nu)$ is incident on an optically pumped vapor. The attenuation of the flux is then

$$\begin{aligned}\Delta\Phi &= \frac{c}{2\pi}\sum_{\omega}[\,|\vec{\mathcal{E}}(\omega,\xi_1)|^2 - |\vec{\mathcal{E}}(\omega,\xi_0)|^2] \\ &= \int \Phi(\omega)d\omega\Big\{\sum_{\omega'\omega''}[\overleftrightarrow{V}(\xi_1\omega';\xi_0\omega)\cdot\vec{e}]\cdot[\overleftrightarrow{V}(\xi_1\omega'';\xi_0\omega)\cdot\vec{e}]^* \\ &\quad\times\exp(i[(k'-k'')\zeta_1-(\omega'-\omega'')t_1]) - 1\Big\} \;.\end{aligned} \tag{30}$$

For optically thin vapors, we can substitute (19) into (30) and retain only linear terms in χ. The attenuation is then

$$\Delta\Phi(t_1) = -\int_0^\infty d\omega\int_{\zeta_0}^{\zeta_1} d\zeta\,\Phi_0(\omega)h(\omega,\zeta,t) \;, \tag{31}$$

where

$$t = t_1 - (1/c)(\zeta_1 - \zeta) \tag{32}$$

and the absorptivity is

$$h(\omega,\zeta,t) = -2\pi ik\,\vec{e}^{\,*}\cdot\langle\overleftrightarrow{\chi}_{\perp}(\omega,\zeta,t)\rangle\cdot\vec{e} + \mathrm{c.c.} \tag{33}$$

Equation (33) may be derived from simple physical considerations. Power is absorbed from a monochromatic light beam because of the work done by the electric field of the light on the oscillating dipole moments of the atoms. The power w absorbed per unit volume is

$$w = \vec{E}\cdot\frac{d\vec{P}}{dt} \;. \tag{34}$$

Differentiating (6), we obtain

$$\frac{d\vec{P}}{dt} = -i\omega\langle\overleftrightarrow{\chi}\rangle\,\vec{\mathcal{E}}\exp[i(\vec{k}\cdot\vec{r}-\omega t)] + \mathrm{c.c.} \tag{35}$$

Any time variation of $\langle\overleftrightarrow{\chi}\rangle$ has been neglected in (35) because the ground-state resonant frequencies are much smaller than the optical frequencies. Since the bandwidth of conventional photodetectors does not extend to optical frequencies, we may substitute (35) into (34) and average over a few optical cycles to obtain

$$\langle w\rangle_{\mathrm{av}} = -i\omega\,\vec{\mathcal{E}}^*\cdot\langle\overleftrightarrow{\chi}\rangle\cdot\vec{\mathcal{E}} + \mathrm{c.c.} \tag{36}$$

Using (29) and the fact that $\vec{\mathcal{E}} = \mathcal{E}\vec{e}$, we obtain

$$\langle w\rangle_{\mathrm{av}} = -2\pi ik\,\vec{e}^{\,*}\cdot\langle\overleftrightarrow{\chi}\rangle\cdot\vec{e}\,\Phi(\nu)d\nu + \mathrm{c.c.} = h\Phi(\nu)d\nu \;. \tag{37}$$

Thus, the absorptivity $h(\omega,\zeta,t)$ is simply the instantaneous power absorbed per unit volume and per unit flux from a light wave of frequency ω.

One can also show that the absorptivity is closely related to the light-absorption operator $\delta\Gamma$ of HM. One finds that for a monochromatic wave

$$h(c/2\pi)|\mathcal{E}|^2 = \omega\hbar N\langle\delta\Gamma\rangle \;. \tag{38}$$

Physically, (38) shows that the rate of absorption of energy from the light wave is just equal to the photon energy times the rate of atomic excitation.

In deriving (31) we assumed that the vapor was optically thin. The same profile function $\Phi_0(\nu)$ and polarization vector $\vec{e}$ can thus be used throughout the volume of the vapor. In the case of optically thick vapors, both the spectral profile and the polarization of the light change in a complicated way as the beam passes through the vapor, and one must use the more general expression (30) instead of (31) to calculate the attenuation of the light beam.

III. POLARIZABILITY OF ALKALI VAPORS

We have shown that the dielectric susceptibility $\langle\overleftrightarrow{\chi}\rangle$ or, equivalently, the dielectric polarizability $\langle\overleftrightarrow{\alpha}\rangle = N^{-1}\langle\overleftrightarrow{\chi}\rangle$ determines the way in which light propagates through a vapor. Because of hyperfine structure, the polarizability of an alkali atom is rather complicated, and in order to facilitate our discussion of the polarizability, it is convenient to write the polarizability operator as the sum of four components:

$$\begin{aligned}\alpha &= \alpha_{\mathrm{eq}} + \alpha_{\mathrm{hfs}}\vec{I}\cdot\vec{J} + i\sum_{ff'}\alpha_{\mathrm{gt}}(ff')\vec{J}(ff')\times \\ &\quad+\sum_{ff'}\alpha_{\mathrm{br}}(ff')\overleftrightarrow{Q}(ff') \;.\end{aligned} \tag{39}$$

The physical significance of each of these components will be discussed in Secs. III A–III D

A. Isotropic Polarizabilities

There are two isotropic components of the polarizability operator: the equilibrium polarizability and the hyperfine-structure polarizability. The equilibrium polarizability $\alpha_{\rm eq}$ is independent of the state of the vapor and is the only component of the polarizability which would be present if the atoms were distributed at random among the sublevels of the ground state. The hyperfine structure polarizability $\alpha_{\rm hfs}\vec{\rm I}\cdot\vec{\rm J}$ has a nonzero expectation value only when some population imbalance $\langle\vec{\rm I}\cdot\vec{\rm J}\rangle$ exists between the upper and lower hyperfine levels of the ground state. Making use of (III. 2), (A15), (A35), and (A36) of HM, we find that we can write the isotropic polarizability operator α_0 as

$$\alpha_0=\alpha_{\rm eq}+\alpha_{\rm hfs}\vec{\rm I}\cdot\vec{\rm J} \quad , \tag{40}$$

where the equilibrium response function is

$$\alpha_{\rm eq}=\frac{1}{2\sqrt{3}\,(2I+1)}\sum_{F_g}(2F_g+1)^{1/2}A_0(F_gF_g) \quad , \tag{41}$$

and the hyperfine-structure response function is

$$\alpha_{\rm hfs}=\frac{2}{\sqrt{3}(2I+1)}\sum_{F_g}\frac{A_0(F_gF_g)}{(2F_g+1)^{1/2}}(-1)^{I+\frac{1}{2}-F_g} \quad . \tag{42}$$

Here,

$$A_0(F_gF_g)=2\sqrt{3}G(2F_g+1)^{1/2}$$
$$\times\sum_{F_e}(2F_e+1)W^2(J_eF_e\tfrac{1}{2}F_g;I1)Z(F_eF_g) \tag{43}$$

[see (III. 3) and (A26) of HM], and

$$G=(\lambda^2r_0f/8\pi^2)(Mc^2/2RT)^{1/2} \quad . \tag{44}$$

The symbol W denotes a Racah coefficient. The plasma dispersion functions[12] $Z(F_eF_g)$ are defined by

$$Z(F_eF_g)\equiv Z(x(F_eF_g)+iy) \quad , \tag{45}$$

$$x(F_eF_g)=\nu^{-1}(Mc^2/2RT)^{1/2}\{[\nu-\nu_{\rm eq}]-[\nu(F_eF_g)-\nu_{\rm eq}]\} \quad , \tag{46}$$

$$y=(Mc^2/2RT)^{1/2}[(1/2\tau+\gamma_c)/2\pi\nu] \quad . \tag{47}$$

All nomenclature is the same as that of HM. In particular, λ is the wavelength of the resonance light, r_0 is the classical electron radius, f is the oscillator strength of the transition, M is the gram molecular weight of the atoms, c is the speed of light, R is the gas constant, T is the absolute temperature, ν is the frequency of the light, $\nu_{\rm eg}$ is the center of gravity of the atomic absorption line, $\nu(F_eF_g)$ is the optical frequency corresponding to a transition between the ground-state level F_g and the excited-state level F_e, τ is the lifetime of the excited state, and γ_c is the collision broadening rate of the optical-absorption line.

The response functions $\alpha_{\rm eq}$ of (41) and $\alpha_{\rm hfs}$ of (42) have been evaluated explicitly for a broadening parameter

$$y=0.5 \quad . \tag{48}$$

The results are shown in Figs. 1–4.

From (33) we find that the equilibrium absorptivity is

$$h_{\rm eq}=4\pi kN\,{\rm Im}\alpha_{\rm eq} \tag{49}$$

and the hyperfine absorptivity is

$$h_{\rm hfs}=4\pi kN\langle\vec{\rm I}\cdot\vec{\rm J}\rangle\,{\rm Im}\alpha_{\rm hfs} \quad . \tag{50}$$

Thus, while the equilibrium absorptivity is independent of the state of the vapor, the hfs absorptivity can serve as a useful monitor of the atomic observable $\langle\vec{\rm I}\cdot\vec{\rm J}\rangle$. Both the equilibrium absorptivity and the hfs absorptivity are independent of the polarization of the light since both originate from isotropic components of the polarizability.

We note that the response function $S_{\rm hfs}(\nu)$ for the hfs light shift of Eq. (4) of Ref. 13 is related to the hyperfine polarizability by the formula

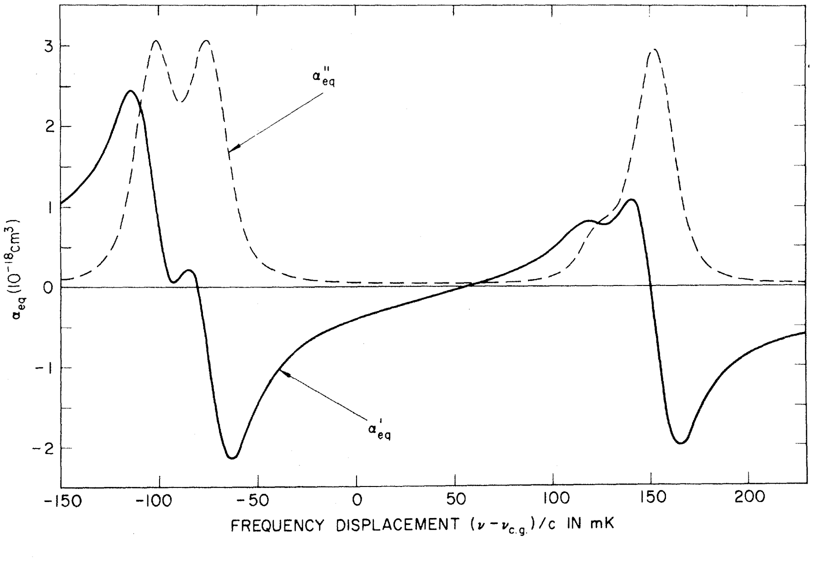

FIG. 1. $\alpha_{\rm eq}$ for D_1 light.

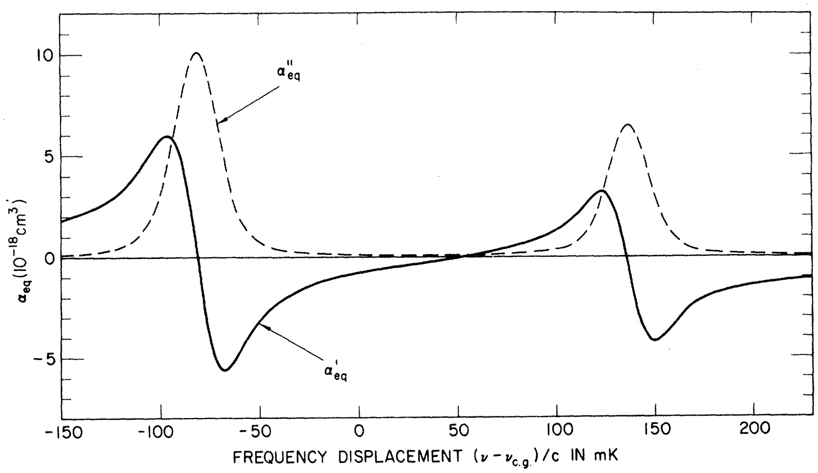

FIG. 2. α_{eq} for D_2 light.

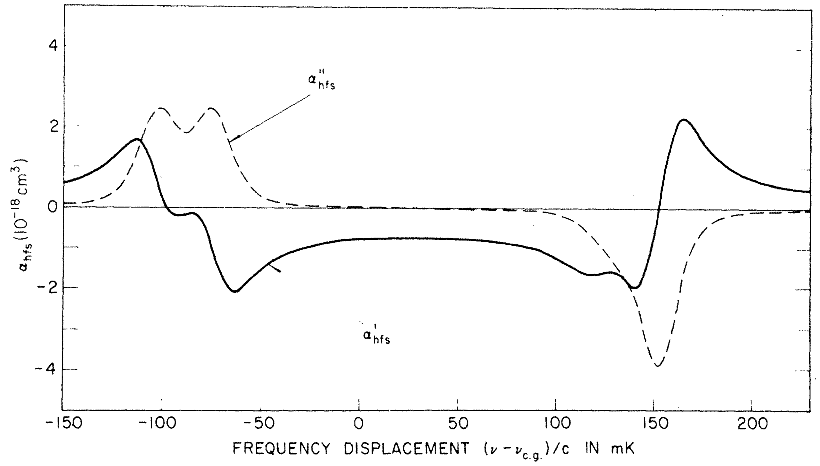

FIG. 3. α_{hfs} for D_1 light.

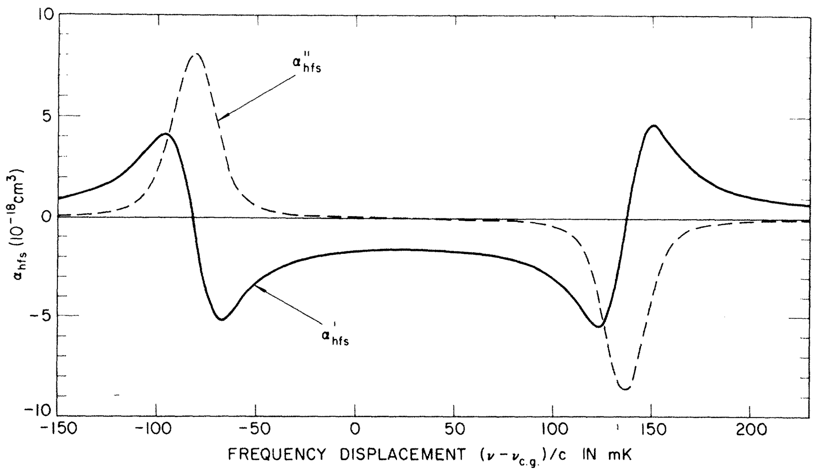

FIG. 4. α_{hfs} for D_2 light.

$$S_{\text{hfs}}(\nu) = -(4\pi/hc)\,\text{Re}\,\alpha_{\text{hfs}} \quad . \qquad (51)$$

B. Gyrotropic Polarizabilities

The gyrotropic polarizabilities of an alkali vapor are anisotropic, and they depend on the expectation values $\langle J(ff')\rangle$ of the electronic angular momentum operator within each hfs level ($f=f'$) and between different hfs levels ($f\neq f'$). The gyrotropic polarizability is important in a wide range of optical-pumping experiments which involve circularly polarized light beams or which utilize the paramagnetic Faraday effect.

Making use of (A26), (A34), and (A16) of HM, we find

$$\alpha_1 = \sum_{F_g F_g'} i\alpha_{gt}(F_g F_g')\,\vec{J}(F_g F_g')\times \quad , \qquad (52)$$

where the frequency response functions are

$$\alpha_{gt}(F_g F_g') = -6G\sum_{F_e}(-1)^{F_e - F_g'}\frac{Z(F_e, F_g')\,(2F_e+1)W(11F_gF_g';1F_e)}{W(1\tfrac{1}{2}F_g I;\tfrac{1}{2}F_g')} \times W(J_eF_e\tfrac{1}{2}F_g;I1)W(J_eF_e\tfrac{1}{2}F_g';I1) \quad . \qquad (53)$$

The projected angular momentum operators are

$$\vec{J}(F_g F_g') = \sum_{\mu\mu'} |F_g\mu\rangle\langle F_g\mu|\vec{J}|F_g'\mu'\rangle\langle F_g'\mu'| \quad . \qquad (54)$$

We have evaluated the gyrotropic response functions (53) for Rb^{87}, and the results are shown in Figs. 5–8.

In the absence of hyperfine coherence, the gyrotropic absorptivity is

$$h_{gt} = 4\pi k N\sum_f \langle\vec{J}(ff)\rangle\cdot\vec{s}\,\text{Im}\,\alpha_{gt}(ff) \quad . \qquad (55)$$

Here the vector $\vec{s}$ is the average photon spin

$$\vec{s} = i\vec{e}\times\vec{e}^{\,*} \quad . \qquad (56)$$

The average photon spin $\vec{s}$ is a unit vector parallel to the beam direction for right-circularly-polarized light, and it is a unit vector antiparallel to the beam direction for left-circularly-polarized light. For all other states of polarization, $\vec{s}$ lies somewhere between these two extreme values. The gyrotropic absorption can serve as a useful monitor of the angular momentum observables $\langle J(ff)\rangle$.

We note that the gyrotropic polarizability is related to the response function $\delta H(F,\nu)$ for the effective magnetic field of Eq. (16) of Ref. 13 by the formula

$$\delta H(F,\nu) = -(2\pi/g_J\mu_0 c)\,\text{Re}\,\alpha_{gt}(FF) \quad . \qquad (57)$$

C. Birefringent Polarizabilities

The birefringent polarizabilities of an alkali vapor are anisotropic, and they depend on the expectation values $\langle\overleftrightarrow{Q}(ff')\rangle$ of the quadrupole operators:

$$\overleftrightarrow{Q}(ff') = \sum_m (-1)^m \overleftrightarrow{Q}_{2m} T_{2-m}(ff') \quad . \qquad (58)$$

Here, $\overleftrightarrow{Q}_{2m}$ is an irreducible basis dyadic defined by (A10) of HM, and $T_{2m}(ff')$ is an irreducible basis operator defined by (A1) of HM. The birefringence of an alkali vapor is negligible when the excited-state hyperfine structure is small compared to the Doppler widths of the atomic absorption lines. However, the birefringence is quite noticeable in rubidium and cesium vapors, where the excited-state hyperfine structure is fairly large.

From (III. 2), (III. 3), and (A26) of HM, we find that the birefringent polarizability is

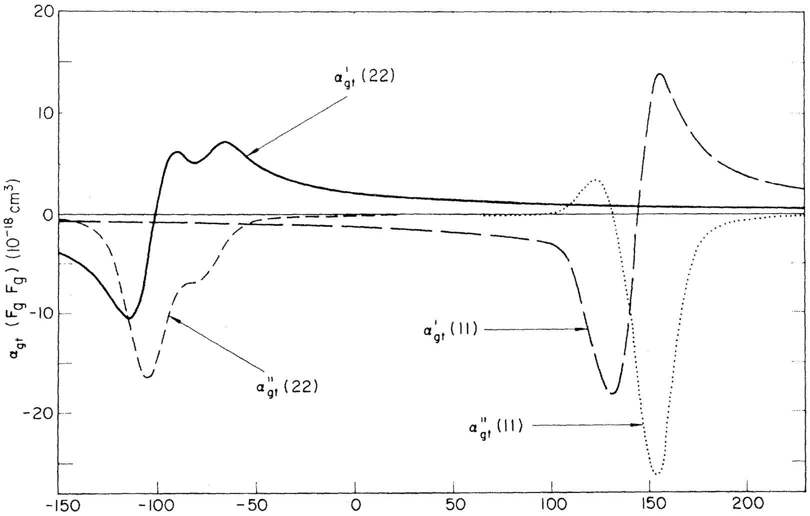

FIG. 5. $\alpha_{gt}(aa)$ and $\alpha_{gt}(bb)$ for D_1 light.

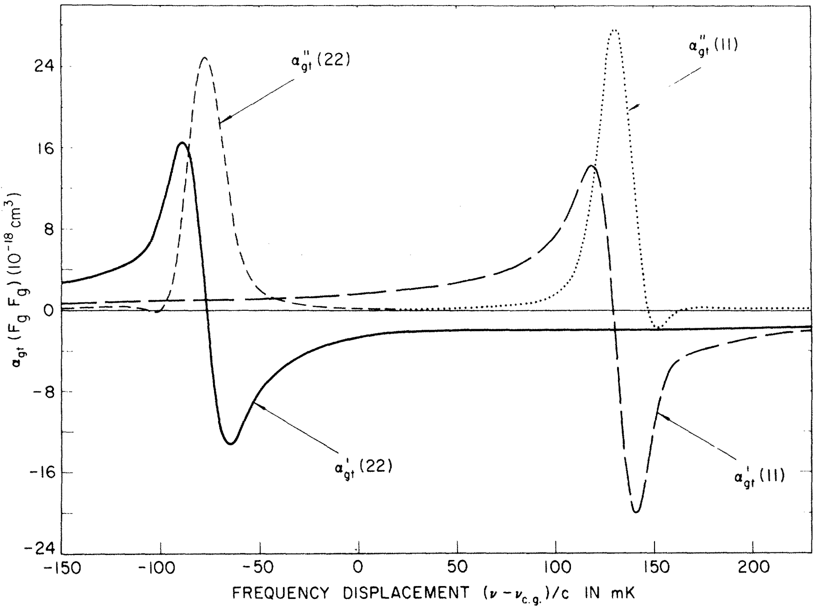

FIG. 6. $\alpha_{gt}(aa)$ and $\alpha_{gt}(bb)$ for D_2 light.

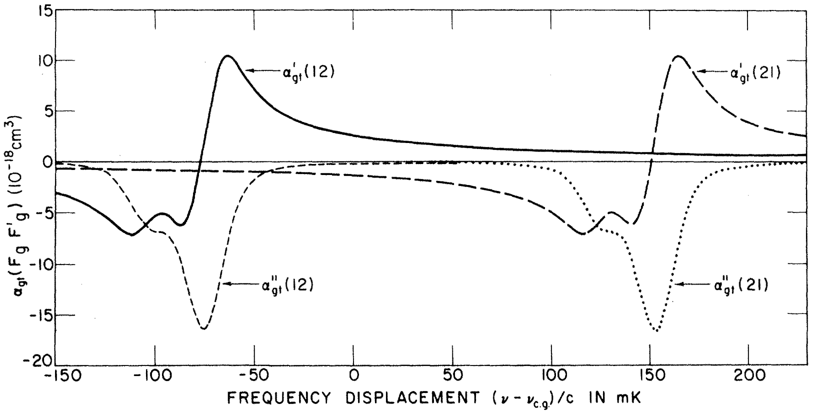

FIG. 7. $\alpha_{gt}(ab)$ and $\alpha_{gt}(ba)$ for D_1 light.

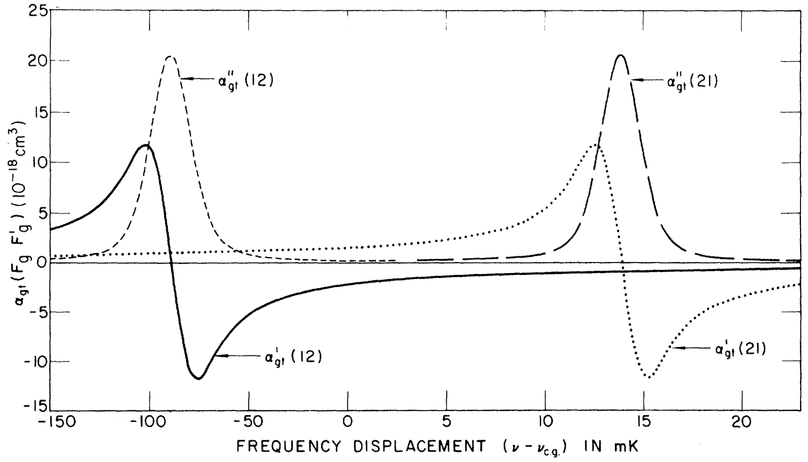

FIG. 8. $\alpha_{gt}(ab)$ and $\alpha_{gt}(ba)$ for D_2 light.

$$\overleftrightarrow{\alpha}_2=\sum_{F_gF_g'}\alpha_{\mathrm{br}}(F_gF_g')\overleftrightarrow{\mathrm{Q}}(F_gF_g')\ , \tag{59}$$

where

$$\alpha_{\mathrm{br}}(F_gF_g')=A_2(F_gF_g')\ =6G\sum_{F_e}(-1)^{F_e-F_g'-1}Z(F_eF_g')$$

$$\times[(2F_g+1)(2F_g'+1)]^{1/2}(2F_e+1)W(11F_gF_g';\ 2F_e)$$

$$\times W(J_eF_e\tfrac{1}{2}F_g;I1)\,W(J_eF_e\tfrac{1}{2}F_g';I1)\ . \tag{60}$$

The birefringent response functions $\alpha_{\mathrm{br}}(22)$ and $\alpha_{\mathrm{br}}(11)$ have been explicitly evaluated for Rb^{87}, and the results are shown in Figs. 9 and 10.

In the absence of hyperfine coherence, we may use (33) to write the birefringent absorptivity as

$$h_{\mathrm{br}}=4\pi kN\sum_f\vec{\mathrm{e}}^*\cdot\langle\overleftrightarrow{\mathrm{Q}}(ff)\rangle\cdot\vec{\mathrm{e}}\,\mathrm{Im}\,\alpha_{\mathrm{br}}(ff)\ . \tag{61}$$

The birefringent absorptivity can serve as a useful monitor of the quadrupole observables.

We note that the birefringent polarizability is related to the frequency response curve $S_2(\nu)$ for tensor light shift for Eq. (22) of Ref. 13.

D. Summary

The polarizabilities of an alkali atom are characterized by certain frequency-response functions, which are shown for Rb^{87} in Figs. 1–10. The complex response functions $\alpha_{\mathrm{gt}}(ff')$ and $\alpha_{\mathrm{br}}(ff')$ $(f\neq f')$, are used when hyperfine coherence is present in the vapor. They measure the production efficiency of upper and lower hfs sidebands. We shall not have occasion to discuss them any further here, but we shall make extensive use of them in a future paper. For all of the other frequency-response functions [i.e., for α_{eq}, α_{hfs}, $\alpha_{\mathrm{gt}}(ff)$, and $\alpha_{\mathrm{br}}(ff)$], the real part of the response function is responsible for phase shifts of the light wave, and the imaginary part is responsible for attenuation. Both real and imaginary components will, in general, cause changes in polarization of the light wave. The light-shift response functions of Ref. 13 can be expressed in terms of the real parts of the polarizability response functions.

The effect of the polarizability of the vapor on light propagation is illustrated in a qualitative way in Fig. 11. As we remarked earlier, the equilibrium polarizability is independent of the state of the vapor. In principle, any two of the remaining three polarizability components could be made zero. The nonequilibrium polarizability of the vapor would then be determined solely by the hfs polarizability, by the gyrotropic polarizabilities, or by the birefringent polarizabilities. Beneath each polarizability component of Fig. 11 we have sketched the wave surface which would result if the nonequilibrium polarizability were determined by that component alone. For the hfs polarizability, the wave surfaces are degenerate spheres. There is no dependence on the direction of propagation or on polarization. For the gyrotropic polarizability, the origins of the wave surfaces, which correspond to σ_+ and σ_- light, are congruent ellipsoids of revolution with the origin at one focus for σ_+ light and at the conjugate focus for σ_- light. For the birefringent polarizability, the wave surfaces are just those of a birefringent crystal. For simplicity, we have sketched the wave surfaces which would result if the vapor behaved like a uniaxial crystal. This is the case, for instance, when

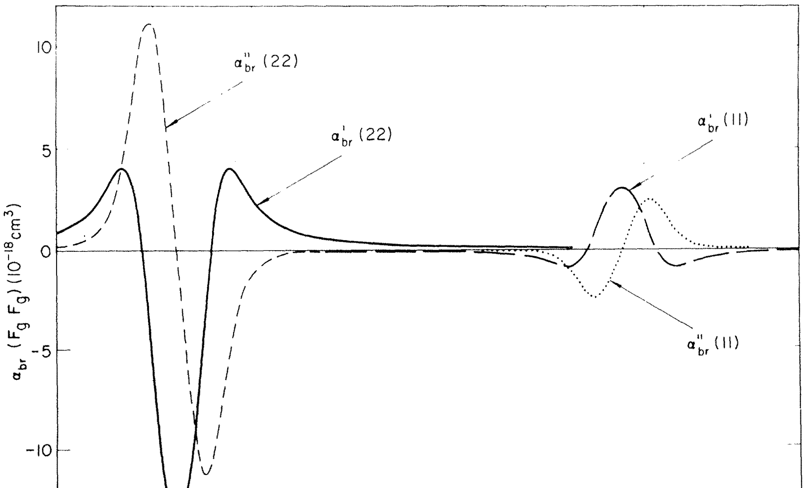

FIG. 9. $\alpha_{\mathrm{br}}(aa)$ and $\alpha_{\mathrm{br}}(bb)$ for D_1 light.

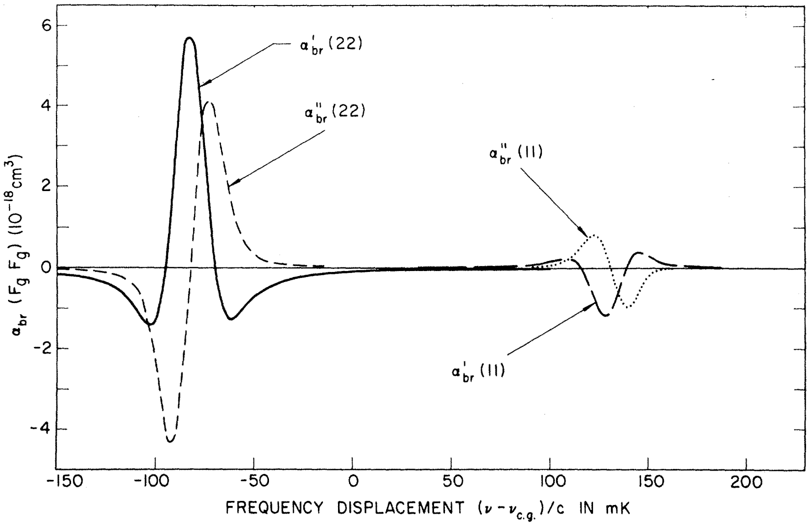

FIG. 10. $\alpha_{br}(aa)$ and $\alpha_{br}(bb)$ for D_2 light.

no coherence exists in the vapor. The wave surfaces are a sphere for ordinary waves which are polarized perpendicular to the axis of the quadrupole operators and an ellipsoid of revolution for the orthogonal polarization, i.e., for the extraordinary waves.

IV. EXPERIMENT

A. Rationale

Both the hfs polarizability and the gyrotropic polarizability of optically pumped vapors have been thoroughly investigated and are well understood. However, the birefringent polarizability is less well known and is frequently ignored. Here, we present the results of some experimental studies of birefringence in optically pumped rubidium vapors.

A crossed-beam experiment, shown in Fig. 12, was used to study the birefringence of rubidium vapor. Isotopically pure rubidium metal was distilled into spherical Pyrex cells, and neon or nitrogen buffer gas at a pressure of about 10 Torr was added before sealing off the cells. The cells were pumped with circularly polarized resonance light from lamps of the corresponding isotope, and the pumping beam was directed along a small magnetic field ($\lesssim$ 1 G), which defined the z axis of a coordinate system. A small rf field of frequency ω was used to induce magnetic resonance between the Zeeman sublevels of the atoms. A probing beam of linearly polarized light passed through the vapor at right angles to the magnetic field. The direction of propagation of the probing beam defined the y axis of the coordinate system. The

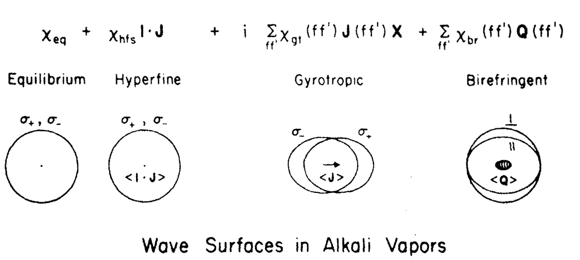

FIG. 11. Wave surfaces and the susceptibility.

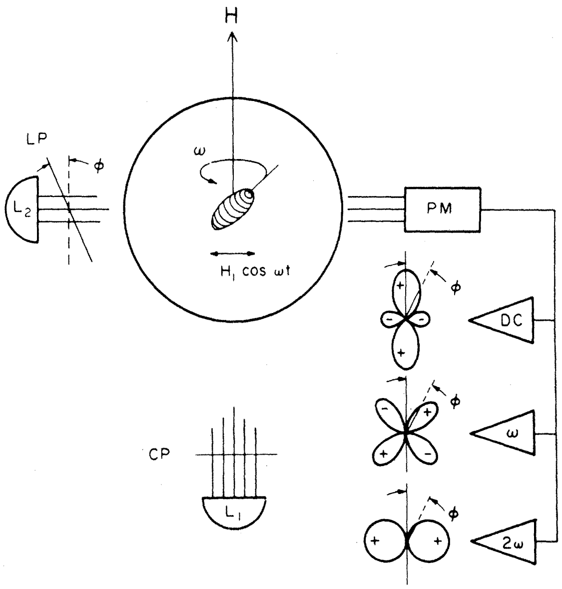

FIG. 12. Experiment on birefringence of Rb vapor.

polarization vector $\vec{e}$ of the probing light made an angle θ with the magnetic field:

$$\vec{e} = \vec{i}_z \cos\theta + \vec{i}_x \sin\theta \quad . \tag{62}$$

No gyrotropic absorption of the linearly polarized probing beam can occur for optically thin vapors, because the average photon spin is zero [see (55)]. However, the equilibrium absorptivity, the hfs absorptivity, and the birefringent absorptivity can contribute to the attenuation of the beam. Both the equilibrium absorptivity and the hfs absorptivity are isotropic and time independent for steady-state conditions. The birefringent absorptivity can be anisotropic and it can be modulated both at the radio frequency and at twice the radio frequency. Thus, in this experiment, any polarization-dependent or oscillatory attenuation of the linearly polarized probing beam must be due solely to the birefringence of the vapor.

Under steady-state conditions the multipole components of the density matrix within each Zeeman multiplet have the form

$$\rho_{LM} = |\rho_{LM}| \exp[i(\pm M\omega t + \alpha_{LM})] . \tag{63}$$

The plus sign applies to the Zeeman multiplet $f = I + \frac{1}{2}$, and the minus sign applies to the multiplet $f = I - \frac{1}{2}$. The amplitudes $|\rho_{LM}|$ and the phases α_{LM} may vary with position within the vapor. For optically thin vapors it is convenient to average these quantities over the pathlength l through the vapor. Thus,

$$|\sigma_{LM}| \exp(i\beta_{LM}) = \frac{1}{l}\int_0^l |\rho_{LM}| \exp(i\alpha_{LM}) d\xi \ . \tag{64}$$

Then, from (31) and (61), one can calculate the birefringent component of the attenuation to be

$$\begin{aligned}\Delta\Phi_{\rm br} = \textstyle\sum_f C[\, &|\sigma_{20}|\, 6^{-1/2}(1 - 3\cos^2\theta) \\ &- |\sigma_{21}| \sin 2\theta \cos(\omega t + \beta_{21}) \\ &- |\sigma_{22}| \sin^2\theta \cos(2\omega t + \beta_{22})] \ ,\end{aligned} \tag{65}$$

where

$$C = 4\pi k N l \int_0^\infty \Phi_0(\omega)\, \mathrm{Im}\, \alpha_{\rm br}(ff) dw . \tag{66}$$

The space-averaged density-matrix amplitudes $|\sigma_{2n}|$, the phase β_{2n}, and the convolution C will, in general, be different for the two different Zeeman multiplets.

B. Observations of Birefringence

In our experiments we did not concern ourselves with the precise values of the quantities $|\sigma_{2n}|$ and β_{2n}, since these depend in a very complicated way on many experimental parameters, such as the pumping-light intensity, the rf field amplitude and frequency, the buffer-gas pressure, the geometry of the cell, etc. Rather, we examined the unambiguously predicted angular dependences: $(1 - 3\cos^2\theta)$ for the dc signal, $\sin 2\theta$ for the signal at the radio frequency and $\sin^2\theta$ for the signal at twice the radio frequency.

For experimental convenience the rf magnetic field was square-wave modulated on and off at a low frequency (≈ 3 Hz). When the rf is turned off, the rf components of the density matrix $\rho_{2M}(M \neq 0)$ decay to zero, and the dc component ρ_{20} assumes some steady-state value which differs from the value when the rf is on. The 3-Hz modulation frequency is low enough for transients in the density matrix to be ignored. Thus, the components ρ_{2M} are essentially square-wave modulated in phase with the square-wave modulation of the rf field.

The dc component $\Delta I_0(\theta)$ of the probing beam was observed by detecting the 3-Hz component of the photodetector output with a phase-sensitive amplifier. The observed angular dependence of the dc component is sketched in Fig. 12. The $\cos^2\theta$ angular dependence, which was predicted by (65), was verified.

To observe the light modulation at the radio frequency ω, the signal from the photodetector was mixed with the rf carrier frequency, and the 3-Hz difference frequency was detected with a phase-sensitive amplifier. The observed angular dependence $I_\omega(\theta)$ of the first harmonic component is sketched in Fig. 12 and is in agreement with the $\sin 2\theta$ variation predicted by (65).

The light modulation at twice the radio frequency was observed by mixing the photomultiplier output signal with the second harmonic of the rf carrier frequency in a balanced mixer. The 3-Hz signal from the balanced mixer was measured with a phase-sensitive detector. The observed angular dependence $I_{2\omega}(\theta)$ is sketched in Fig. 12. The $\sin^2\theta$ angular dependence predicted by (65) was verified.

Signals similar to those sketched in Fig. 12 were observed in Rb^{87} vapor with both D_1 and D_2 probing beams from a Rb^{85} lamp. The D_1 probing beam gave a larger signal, as was to be expected since the birefringent polarizability is larger for D_1 light than for D_2 light (see Figs. 9 and 10).

With a Rb^{87} probing beam, we observed signals which were similar to but very much smaller than those for a Rb^{85} probing beam. This is understandable since a typical Rb^{87} lamp profile overlaps roughly equal positive and negative portions of the response curves (see Fig. 13), and the convolution (66) becomes almost zero. The Rb^{85} spectral profile is asymmetric with respect to the Rb^{87} response curve, and a large convolution results. By inserting a heated Rb^{85} filter cell between the Rb^{87} probing lamp and the Rb^{87} absorption cell it was possi-

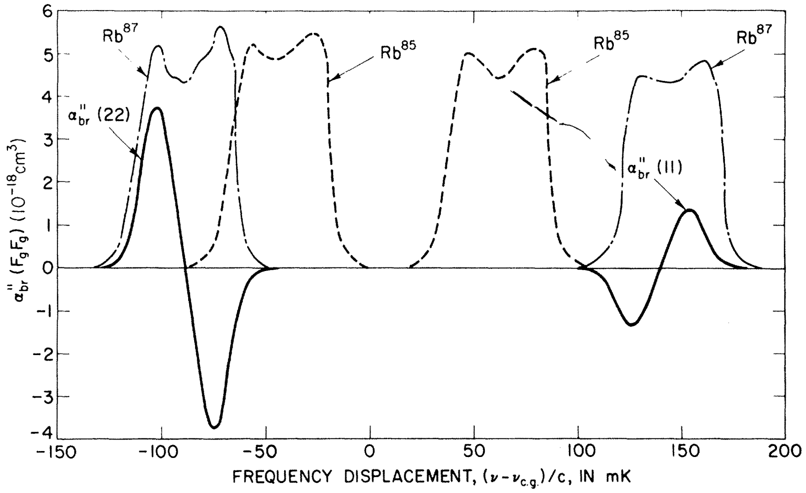

FIG. 13. Overlap of $\Phi(\nu)$ with $\alpha_{br}(\nu)$.

ble to make the birefringent signal much larger. Since the Rb^{85} filter cell selectively absorbed part of the Rb^{87} spectral profile, the modified profile was no longer symmetric with respect to the Rb^{87} response curves, and the convolution (66) was no longer almost equal to zero.

Essentially the same features just described for optically pumped Rb^{87} vapor were also observed for optically pumped Rb^{85} vapor. However, all Rb^{85} signals were significantly weaker than the corresponding ones for Rb^{87} vapor. This is to be expected since the smaller excited-state hyperfine structure of Rb^{85} leads to smaller birefringent polarizabilities.

When the linear polarizer was removed from the probing beam of Fig. 8, signals at the rf were barely observable, while signals at twice the rf were quite strong. These observations are in complete accord with the predictions of (65). We may regard an unpolarized light beam as being composed of two uncorrelated light beams, linearly polarized at right angles to each other. Suppose that the two polarization vectors make angles of θ and $\theta+\frac{1}{2}\pi$ with the magnetic field. According to (65), the first harmonic component will be proportional to

$$I_\omega \propto \sin 2\theta + \sin 2(\theta+\tfrac{1}{2}\pi) = 0 \quad , \tag{67}$$

so no first-harmonic modulation of the unpolarized probing beam should exist. In practice, the direction of the probing beam is never precisely perpendicular to the magnetic field, and a slight degree of polarization is introduced into the beam by lenses and cell walls. Therefore, a very small first-harmonic component is still observed when the linear polarizer is removed.

However, according to (65), the second-harmonic component should be proportional to

$$I_{2\omega} \propto \sin^2\theta + \sin^2(\theta+\tfrac{1}{2}\pi) = 1 \quad , \tag{68}$$

and, in agreement with experiment, a strong second harmonic should occur.

C. Crossed Polarizer and Analyzer

A number of experiments were carried out with a linear polarizer at an angle θ with the magnetic field and a linear analyzer at an angle $\theta+\frac{1}{2}\pi$ with the magnetic field. These experiments with "crossed polarizers" make use of the change in polarization of a light beam which occurs when the beam passes through an optically pumped vapor. The polarization vector $\vec{e}$ of the polarizer is given by (62), and the polarization vector $\vec{u}$ of the analyzer is

$$\vec{u} = -\vec{i}_z \sin\theta + \vec{i}_x \cos\theta \quad . \tag{69}$$

The electric field amplitude of a given monochromatic component of the polarized incident light beam is

$$\vec{\mathcal{E}}_0 = |\mathcal{E}_0|\,\vec{e} \quad . \tag{70}$$

After the beam passes through an optically thin vapor and the analyzer, the amplitude will have been transformed into [see (16)]

$$\vec{\mathcal{E}}_d = \vec{u}\vec{u}\cdot V\vec{\mathcal{E}}_0 \quad . \tag{71}$$

Substituting (70) and (19) into (71), we obtain

$$\vec{\mathcal{E}}_d = \vec{u}\{2\pi i k l \vec{u}\cdot\langle\overleftrightarrow{\chi}\rangle\cdot\vec{e}\}\mathcal{E}_0 \quad . \tag{72}$$

The spectral intensity at the photocathode is then

$$\begin{aligned}\Phi_d(\omega)d\omega &= c|\mathcal{E}_d|^2/2\pi \\ &= 4\pi^2(kl)^2|\vec{u}\cdot\langle\overleftrightarrow{\chi}\rangle\cdot\vec{e}|^2\,\Phi(\omega)d\omega \quad .\end{aligned} \tag{73}$$

From (73) and (39) we find that the total intensity at the photocathode is

$$\Phi_d(\nu) = 4\pi^2 (klN)^2 \int \Phi_0(\nu) d\nu \times \sum_f \left| \{ \langle J_Y \rangle \alpha_{\mathrm{gt}} + ([3/2(6)^{1/2}] \rho_{20} \sin 2\theta + \mathrm{Re}\rho_{21} \cos 2\theta + \mathrm{Re}\rho_{22} \sin 2\theta) \alpha_{\mathrm{br}} \} \right|^2 . \tag{74}$$

One can see from (72) that the signal from a crossed-polarizer experiment is much more difficult to interpret than that from a single-polarizer experiment. Both the gyrotropic and the birefringent polarizabilities contribute, and the signals depend quadratically instead of linearly on the density-matrix components. For optically thin vapors, the dimensionless quantities of the form

$$x = 2\pi klN |\alpha| \ll 1 \tag{75}$$

are very small, and the crossed-polarizer flux is on the order of $x^2\Phi_0$, where Φ_0 is the initial flux of the light beam. The attenuated flux in a single polarizer is on the order of $x\Phi_0$. Hence, the crossed-polarizer signals should be weaker by a factor of x than single-polarizer signals. A further practical complication is that it is very difficult to get truly crossed polarizers. Without special precautions, a small amount of light passes through the polarizer because of imperfections in the polarizers, the angular divergence of the beam, and the polarizing action of the glass walls of the cell. To account for these effects, some terms which are linear in the susceptibility should be included in (74).

Because of the quadratic dependence of the crossed-polarizer signals on the polarizabilities, third- and fourth-harmonic light modulation, as well as very complicated angular dependences, can occur. In view of the complexities and uncertainties which attend the interpretation of a crossed-polarizer experiment, no systematic studies were made. However, sizable signals were found and, as an example, we reproduce in Fig. 14 the dc signals which were observed in Rb^{87} vapor with a Rb^{87} probing beam. The observed angular dependence can be accounted for in a qualitative way by the use of (74).

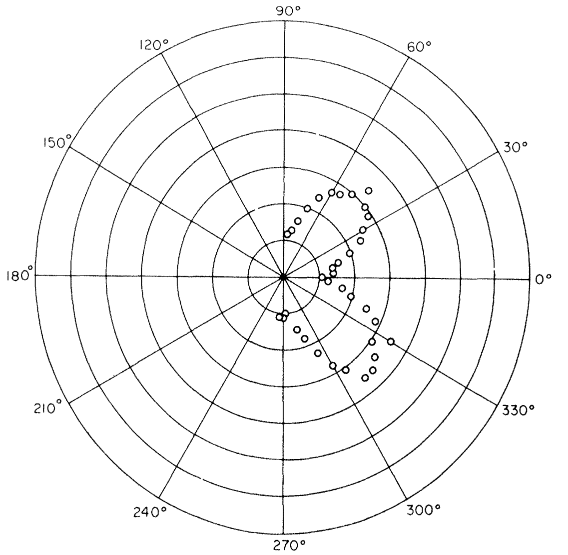

FIG. 14. Crossed-polarizer signals. The angle is that which is between the incident polarizer and the magnetic field.

ACKNOWLEDGMENTS

We would like to thank the staff of the Columbia Radiation Laboratory for their assistance in this work. We are particularly grateful to R. Brignoli for help in the experiments, and to J. Clendenin for computer programming.

---

*Work supported by the Joint Services Electronics Program (U. S. Army, U. S. Navy, and U. S. Air Force) under Contract No. DAAB07-69-C-0383.

†Present address: Indian Institute of Technology, Kanpur-16 (U. P.) India.

[1] W. E. Bell and A. L. Bloom, Phys. Rev. 107, 1559 (1957).

[2] M. A. Bouchiat, J. Phys. 26, 415 (1965).

[3] M. A. Bouchiat and F. Grossetête, J. Phys. (Paris) 27, 353 (1966).

[4] B. S. Mathur, Columbia Radiation Laboratory progress Report No. 17, 1968 (unpublished).

[5] B. S. Mathur, H. Tang, R. Bulos, and W. Happer, Phys. Rev. Letters 21, 1035 (1968).

[6] W. Happer and B. S. Mathur, Phys. Rev. 163, 12 (1967).

[7] C. Cohen-Tannoudji and F. Laloë, J. Phys. (Paris) 28, 505 (1967); 28, 722 (1967); F. Laloë, M. Leduc, P. Minguzzi, *ibid.* 30, 277 (1969); 30, 341 (1969).

[8] W. Happer, *Optical Pumping Theory* (Gordon and Breach, New York, 1969), Vol. XIc.

[9] C. L. Tang and B. D. Silverman, *Physics of Quantum Electronics*, edited by P. L. Kelley, B. Lax, and P. E. Tannenwald (McGraw-Hill, New York, 1966), p. 280.

[10] F. A. Jenkins and F. A. White, Fundamentals of Physical Optics (McGraw-Hill, New York, 1937).

[11] W. E. Bell and A. L. Bloom, Phys. Rev. Letters 6, 280 (1961).

[12] B. D. Fried and S. D. Conte, *The Plasma Dispersion Function* (Academic, New York, 1961).

[13] B. S. Mathur, H. Tang, and W. Happer, Phys. Rev. 171, 11 (1968).